

## OBSERVATIONS OF INTERFACIAL DAMAGE IN THE FIBER BRIDGED ZONE OF A TITANIUM MATRIX COMPOSITE

DREW BLATT  
Materials Directorate  
Wright Laboratory  
WPAFB, OH 45433-7178, USA

PRASANNA KARPUR and DAVID A. STUBBS  
University of Dayton Research Institute  
300 College Park Avenue  
Dayton, OH 45469-0120, USA

THEODORE E. MATIKAS  
NRC Fellow, Materials Directorate  
Wright Laboratory  
WPAFB, OH 45433-7178, USA

(Received April 16, 1993)

(Revised June 24, 1993)

### Introduction

As a matrix crack progresses through a continuous-fiber reinforced composite, a fiber bridged zone often develops in the crack wake. Attempts to model this behavior (1-4) usually begin by analyzing the unit cell shown in Fig. 1. Inherent to this unit cell is the presence of a sliding frictional stress ( $\tau$ ) acting over a slip region with a characteristic length,  $l$ . However, in modeling of fiber debonding and pullout, Hutchinson and Jensen (5) considered a similar unit cell with  $l$  divided into a frictional sliding zone and a zero-friction zone. This reduced friction or friction free zone is a physical possibility during long duration fatigue cycling. Their model also includes the effect of temperature changes on the magnitude of sliding resistance at the fiber/matrix interface.

The early shear lag models (1, 2) considered static loading whereas, recent shear lag formulations (6) also account for cyclic crack opening. During cyclic loading the interface properties (e.g., frictional shear stress) change; typically the frictional sliding resistance decreases when a composite or a push-out sample is subjected to reversed cyclic loading (7-9). Eventually though the frictional sliding resistance reaches a steady-state condition. In reviewing current fiber bridging models, Bakuckas and Johnson (10) claimed that the frictional shear stress in a debonded region is a function of crack length, applied stress, and distance along the debond length.

Environment can also influence the fiber/matrix interfacial integrity. Marcus (11) and Park and Marcus (12) reported on diffusion of oxygen and sulfur along the interface and into the matrix of Ti-6Al-4V reinforced with SiC and B<sub>4</sub>C/B continuous fibers. Samples were thermally cycled in air between room temperature and 550 °C for one day. The samples had high concentration peaks of oxygen at the interface near the exposed surface and diffusion of oxygen some distance into the interface. Two one-dimensional analyses were conducted: one of the rapid diffusion down the interface; and one of the slow diffusion into the bulk matrix material. From these analyses, Marcus (11) concluded that the sulfur diffusion along the interface was about five orders of magnitude greater than the coupled diffusion into the matrix and the diffusion rate along the interface was temperature dependent.

Two thermal fatigue studies (13, 14) report that titanium matrix composites subjected only to thermal cycles developed surface matrix cracks that grew inward towards the fiber. Once at the fiber-matrix interface, the cracks allowed the environment to attack the interface. The thermal fatigue studies (13, 14) indicate that once matrix cracks reached the interface the environmental attack on the fiber coatings is severe. Revelos and Smith (14) also performed thermal cycling tests in an inert atmosphere and found that no matrix cracking occurred on the specimens tested. With this in mind, it becomes apparent that within a fiber bridged region of a fatigue crack growth specimen the opportunity for accelerated degradation of the fiber-matrix interface subjected to elevated temperatures is present. The debond region necessarily associated with the fiber bridged zone presents a clear path for environmental encroachment.

This paper presents the results of both nondestructive and destructive evaluations performed after a fatigue crack growth test run under out-of-phase thermomechanical fatigue (TMF) conditions. Post test evaluation indicates that the damage along the fiber-matrix interface in the fiber bridged zone in the TMF specimen is of a much greater scale than the slip region predicted by the shear lag models in their current form.

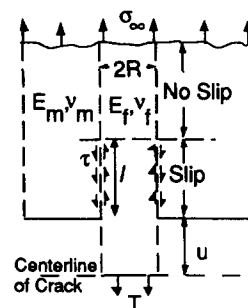


FIG. 1. Typical unit cell used in shear lag analysis.

### Experiments

To evaluate the environmental attack on the fiber-matrix interfacial region, a thermomechanical fatigue crack growth test was performed on a single edge notch specimen with clamped ends (15). The specimen was a 4-ply, unidirectional, fiber reinforced titanium with a fiber volume fraction  $\approx 36\%$ . The matrix material was Ti-15Mo-3Nb-3Al-0.2Si (wt %), and the reinforcing fibers were silicon carbide, SCS-6. The width and thickness was 25.37 mm and 0.96 mm, respectively and the initial notch length-to-width ratio was 0.30. The specimen was gripped such that the height-to-width ratio was 4.0. The specimen was cycled at a frequency of 0.0056 Hz between 150-650 °C out-of-phase with an applied constant stress range of 122.3 MPa and a stress ratio (R) of 0.1. The load was applied parallel to the fiber direction.

During the test, the specimen developed two matrix cracks from the corners of the diamond-saw notch. The cracks then propagated perpendicular to the fiber and load direction. Crack length was monitored using electric potential drop (EDP) over the life of the specimen. The crack length was also verified through periodic optical measurements of the surface cracks. The crack growth rate increased initially as the matrix cracks grew away from the notch. As the matrix cracks continued across the specimen the crack growth rate began to decrease. This type of behavior in composite crack growth is indicative of a developing fiber bridged zone in the wake of the matrix crack. Since the bridging zone continued to develop across the entire matrix crack region, the crack growth rate further diminished to a point that only small crack extensions (0.1 mm) occurred over long periods (6 days). Upon reaching this slow growth rate, the test was terminated prior to fracture after the specimen was subjected to 14,612 thermomechanical cycles over a period of 36 days.

### Nondestructive Evaluation

To determine the extent of internal damage to the specimen after the fatigue crack growth test, the specimen was subjected to a modified ultrasonic through-transmission C-scan technique called reflection plate inspection. This technique (16) used a 10 MHz center frequency broadbanded transducer, 12.7 mm in diameter and spherically focused at 75 mm resulting in a 0.9 mm (-6dB) spot size. Typical step sizes (distance between adjacent X, Y data acquisition locations) were 0.25 - 0.50 mm. This type of ultrasonic technique is often used to assess the quality of consolidation and to detect defects in metal matrix composites (17).

The reflector plate C-scan of the TMF specimen shown in Fig. 2a, shows a large, well defined, region of great ultrasonic attenuation. Some of the ultrasonic attenuation can be caused by dissipation of the acoustic signal in the specimen due to internal damage in the material. Previous work by Stubbs (17) showed that regions of high or even moderate attenuation in a composite were either due to damage caused during the manufacturing process or during mechanical testing. The large, dark region in Fig. 2a is partly explained by the presence of a fiber bridged zone, i.e. debond length, but more importantly by the degradation of the fiber-matrix interface as a result of exposure to the elevated temperatures and thus subject to environmental attack. It should be pointed out that the damage indicated by the reflector plate C-scan extends only as far as the longest surface matrix crack length. This suggests that no damage precedes the crack and environment does not play a role until the debonded fiber-matrix interface is exposed via crack bridging. Interestingly, the fiber ends exposed by the notch do not show the large scale damage (fiber-matrix interfacial degradation) that the continuous load-bearing fibers do beyond the notch. This suggests that damage accumulates more rapidly along a fiber that carries load and is exposed to the environment compared to an exposed unloaded fiber. The two dark spots to either side of the mushroom shaped region are indications of damage that accumulated from control thermocouples spot welded to the surface of the specimen.

An additional ultrasonic evaluation was performed. A novel approach developed by Karpur, et al (18) based on scanning acoustic microscopy (SAM) was used to scan the outside layers of the specimen after the test was terminated. The operating principle of a SAM transducer is based on the production of surface acoustic waves (SAW) propagating due to a combination of the high curvature of the focusing lens of the transducer and the defocus of the transducer into the sample (19). Depending on the defocus (20), the SAM technique can be used either to map the interference phenomenon in the first layer of subsurface fibers or to map the surface and subsurface features (reflectors) in the sample. The scan of the TMF specimen was performed with a 50 MHz transducer with a focal spot size of about 15 microns and a depth of penetration of about 140 microns.

It was shown for the first time (20) that the SAM technique (Fig. 2b) was able to image the interfacial degradation phenomenon. The depth of penetration and the resolution of the scanning acoustic microscope are sufficient to detect the interfacial changes as evidenced by the visualization of each fiber in the outside layer of the 4-ply composite. The scan from the SAM method supports the idea that environment assisted damage along the fiber-matrix interface is noticeably accelerated when the fiber is carrying load, in this case cyclic load. Note the fibers along the notch edge (stress free surface) do not show as much damage as those continuous load-bearing fibers in the

fiber bridged zone. Another distinct feature shown in Fig. 2b is that the damage to the fiber-matrix interface does not precede the matrix crack tip. That is, the damage only occurred after the matrix crack progressed past an unbroken fiber and exposed the interface to environmental attack. Additional cracks shown on either side of the two primary matrix cracks were the result of thermocouple spot welds on the surface of the specimen prior to testing. Surface cracks initiated at the spot welds and as expected allowed environmentally assisted damage to occur as the surface cracks grew perpendicular to the fibers.

### Metallographic Analysis

To clarify the findings of the through-transmission and scanning acoustic microscope techniques, one side of the specimen was etched using a saturated solution of tartaric acid in 10% bromine and methanol. Matrix etching was stopped after the first layer of fibers was exposed. The photomicrograph shown in Fig. 2c illustrates a darkened region that clearly resembles the ultrasonic signature of the reflector plate C-scan (Fig. 2a) and the SAM (Fig. 2b) techniques. From the photomicrograph, it becomes obvious that the particular SAM technique used (18, 20) is capable of providing a nondestructive method for tracking interfacial damage. Again, it is clear from Fig. 2c that the amount of damage along a fiber-matrix interface is directly influenced by the load carrying capability of the fiber and the amount of time that the fiber was exposed to the environment.

The etching solution was chosen so that little harm would be done to the fiber coating during the etching process. Figure 3 represents a high magnification view of the fibers near the machined notch. Region "A" shows oxidized diffusion products that are spalling off the fibers. In certain areas of region "A", the silicon carbide is actually visible underneath the discolored diffusion products. This means that the two carbon coatings normally present on SCS-6 fibers have off-gassed in the presence of the elevated temperatures and environmental exposure. This is similar to the observations made by Revelos, et al (21) during thermal fatigue studies of the same material. While the carbon coatings may be gone, it does not necessarily imply that the fibers are "loose" in the matrix. Residual stresses in the matrix, present after consolidation, still exert a reduced clamping force onto the fiber. The reduction in clamping force along with repeated sliding of the fiber against the matrix will lead to reductions in  $\tau$  as discussed above.

Using an SEM with a microprobe, diffusion products in region "B" were found to be typical of those at the fiber-matrix interfacial region (22) of other titanium based composites reinforced with silicon-carbide fibers. The etching solution would not attack regions that were oxidized, such as crack faces, or diffusion products; again, Revelos, et al (21) observed similar behavior. Interestingly, the damage and discoloration along the fiber-matrix interface abruptly change to unaffected or undamaged interfacial coating. That is, the darkened region was well defined when viewed under higher magnification and no extended transition region from damaged to undamaged coating was evident.

### Discussion

As discussed earlier, the damage along the interface shown in Fig. 2c is only present where the fiber interface was exposed either at the notch or along a matrix crack; no damage precedes the matrix crack tip. While the fiber is still surrounded by matrix, it is isolated and protected from any environmental attack. As the matrix crack advances toward and beyond an unbroken fiber the opportunity for environmental attack presents itself. It is speculated that after the initial exposure to the environment, the damage to the fiber-matrix interface is influenced by the type of environment and/or temperature, the amount of stress carried by the fiber, whether or not the fiber fractures, and the time of exposure. For example, a reflector plate C-scan of a room temperature fatigue crack growth specimen tested under similar loading conditions showed no damage along the fiber interfaces like Fig. 2a does. Additionally, Karpur, et al (20) observed interfacial damage in a titanium based composite subjected to isothermal fatigue crack growth conditions.

It is unclear whether, in the TMF specimen, the entire damage length along the interface in the bridged zone can be classified as a slip region. The slip region, illustrated in Fig. 1, is a principal feature in the shear lag models (1, 2) that analyze the bridging phenomenon commonly found in ceramic and metal matrix composites. The theory is developed around the fundamental notion that a bridged fiber must have a characteristic length that displaces relative to the surrounding matrix. The slip region, therefore, allows the environment to not only attack at the fracture surface but progress along the fiber-matrix interface as the slip region develops. The point of discussion then becomes whether the environmental attack extends beyond the slip region, represented by  $l$  in Fig. 1, or if the slip region and the environmental damaged interface coincide with one another.

The slip length can be determined based on the shear lag model by Marshall, et al (1) using

$$l = [uRE_f / \tau(1 + \eta)]^{1/2} \quad (1)$$

where  $u$  is the crack opening displacement,  $R$  is the fiber radius,  $E_f$  is the modulus of the fiber,  $\tau$  is the frictional sliding stress, and  $\eta = E_f V_f / E_m V_m$ . The value of  $\tau$  has been reported in the range of 5 to 250 MPa (4) depending on matrix material and test conditions. The values used in Eq. 1 are given in Table 1. The value of  $\tau = 20$  MPa was chosen to represent a steady-state value of frictional shear stress after sufficient fatigue cycles; it represents the low side of the range of  $\tau$ 's reported above. The slip length,  $l$ , at the notch using Eq. 1 and the loading conditions imposed during the TMF test is equal to 2.3 mm, where as the darkened length measured along the first continuous fiber at the notch is almost 7 mm. Clearly there is a significant difference in the two distances that is not yet fully explained.

Work is currently underway to systematically understand the separate and combined effects of temperature and load on the integrity of the fiber-matrix interface. The preliminary findings support the idea that fiber-matrix interface exposed to temperature alone does degrade but at a much slower rate than one with load and temperature combined.

TABLE 1  
Constants used in Eq. 1 to determine slip length at notch.

| $u$ (@ $x=7.5\text{mm}$ ) ( $\mu\text{m}$ ) | $R$ ( $\mu\text{m}$ ) | $E_f$ (GPa) | $\tau$ (MPa) | $\eta$ |
|---|-----------------------|-------------|--------------|--------|
| 11.6  | 71                    | 400         | 20           | 1.99   |

#### Acknowledgment

This research was conducted at the Materials Directorate, Wright Laboratory, Wright-Patterson Air Force Base, OH. Mr. Blatt is supported by the U.S. Air Force Senior Knight Program. Dr. Karpur is supported by contract number F33615-89-C-5612. Mr. Stubbs is supported by contract number F33615-91-C-5606.

#### References

1. D.B. Marshall, B.N. Cox and A.G. Evans, *Acta Metallurgica*, 33, 2013, (1985).
2. L.N. McCartney, *Proc. R. Soc. Lond.*, A409, 329, (1987).
3. B.N. Cox and D.B. Marshall, *Fatigue Fracture Engineering Materials and Structures*, 14, 847, (1991).
4. D.L. Davidson, *Metall. Trans. A*, 23A, 865, (1992).
5. J.W. Hutchinson and H.M. Jensen, *Mechanics of Materials*, 9, 139, (1990).
6. R.M. McMeeking and A.G. Evans, *Mech. Mater.*, 9, 217, (1990).
7. D.B. Marshall, M.C. Shaw and W.L. Morris, *Acta Metall Mater*, 40, 443, (1992).
8. K.S. Chan, *Acta Metall. Mater.*, 41, 761, (1993).
9. C.H. Hsueh, *Mater. Sci. Eng.*, A130, L11, (1990).
10. J.G. Bakuckas and W.S. Johnson, Langley Research Center, NASA TR 107588, (1992).
11. H.L. Marcus, Final Technical Report AFOSR-TR-84-0812, (1984).
12. Y.H. Park and H.L. Marcus, in *Mechanical Behavior of Metal-Matrix Composites*, J. E. Hack, M. F. Amateau, Eds., TMS-AIME (1983).
13. S.M. Russ, *Metall. Trans. A*, 21A, 1595, (1990).
14. W.C. Revelos and P.R. Smith, *Metall. Trans. A*, 23A, 587, (1992).
15. D. Blatt, R. John and D. Coker, *submitted to Engng. Fract. Mech.*, , , (1993).
16. J. Krautkramer and H. Krautkramer, *Ultrasonic Testing of Materials.*, (Springer-Verlag, New York). (1990).
17. D.A. Stubbs, S.M. Russ and P.T. MacLellan, submitted to ASTM's Second Symposium on Cyclic Deformation, Fracture, and Nondestructive Evaluation of Advanced Materials, (1992).
18. P. Karpur, T.E. Matikas, M.P. Blodgett, D. Blatt and J.R. Jira, *to be submitted to Mater. Evaluatn.*, (1993).
19. C.F. Quate, A. Atalar and H.K. Wickramasinghe, *Proceedings of the IEEE* vol. 67, pp. 1092, (1979).
20. P. Karpur, T.E. Matikas, M.P. Blodgett, J. Jira and D. Blatt, Symposium on Special Applications and Advanced Techniques for Crack Size Determination Atlanta, Georgia), (1993).
21. W.C. Revelos, J.W. Jones and E.J. Dolley, *submitted to Met. Trans. A*, (1993).
22. G. Das and F.H. Froes, Sixth World Conference on Titanium Les Editions de Physique, Titanium, Science Technology and Applications, (1988).

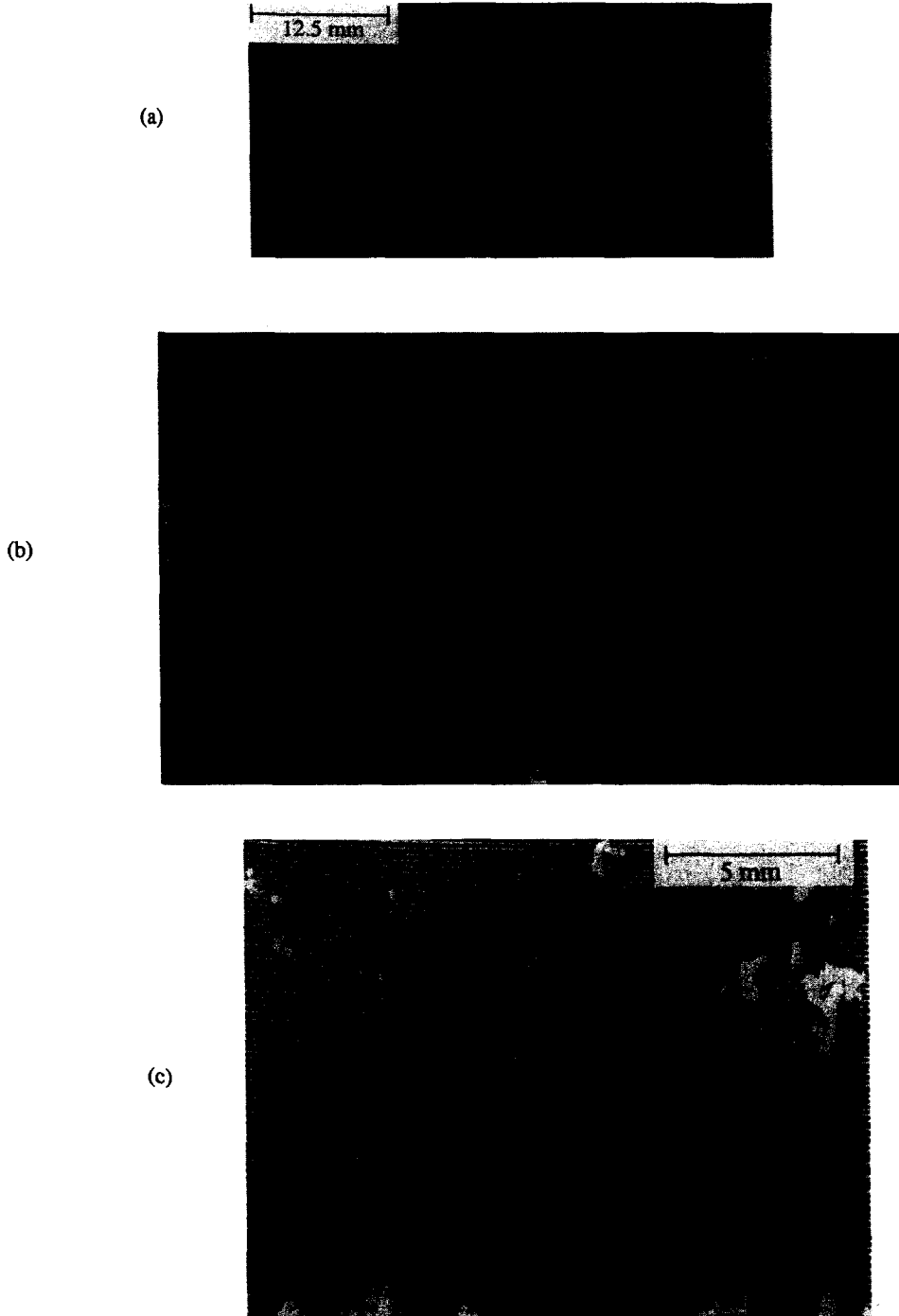


FIG. 2. Damage along fiber-matrix interface as evident by (a) reflector plate ultrasonic C-scan (mirror image of (b) and (c)) (b) scanning acoustic microscope and (c) metallographic analysis.

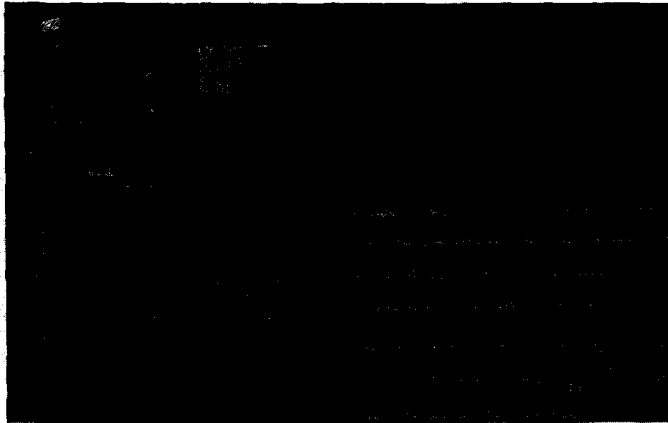


FIG. 3. Photomicrographs of fiber coating spalling off fiber in degraded region "A" and intact fiber coating in unaffected zone "B".